J|A|C|S COMMUNICATIONS

Published on Web 04/14/2009

Star-Shaped Multichromophoric Arrays from Bodipy Dyes Grafted on Truxene Core

Stéphane Diring,[†] Fausto Puntoriero,[‡] Francesco Nastasi,[‡] Sebastiano Campagna,*[,‡] and Raymond Ziessel*[,†]

Laboratoire de Chimie Moléculaire, ECPM-CNRS, 25 rue Becquerel, 67087 Strasbourg Cedex 02, France, and Dipartimento di Chimica Inorganica, Chimica Analitica e Chimica Fisica, Università di Messina, 98166 Vill. S. Agata, Messina, Italy

Received February 27, 2009; E-mail: campagna@unime.it; ziessel@chimie.u-strasbg.fr

Supramolecular multichromophoric systems containing photoactive subunits are extensively investigated for both fundamental and applicative reasons.[1] Several such reasons are linked to the possibility for properly designed multichromophoric architectures to behave as light-harvesting antennae for application in solar energy conversion devices.[2]

Difluoroborondipyrromethene species (Bodipy) are quite interesting dyes, since they exhibit strong visible absorption and intense luminescence, which can be tuned in energy and lifetime by incorporating suitable substituents on the organic framework.[3−5] Truxene species are recently characterized chromophores,[6] which can play the role of photoactive cores for multichromophoric systems.[7] Bodipy dyes and truxene species are compatible systems from a photochemical point of view, since they absorb at different wavelengths (essentially UV region for truxene species, visible for the Bodipy dyes), so they can be addressed separately, to a large extent.

By taking advantage of the structural and photophysical properties of truxene derivatives and Bodipy molecules, we prepared a novel star-shaped supramolecular system containing three *different* bodipy dyes logically arranged around a truxene core. This is the first time that Bodipy and truxene chromophores are linked into the same (super)molecule. The structural formula of the novel species is shown in Scheme 1, together with the formulas of individual dyes and bichromophoric models. Owing to the different Bodipy species used to prepare **1**, four *different* chromophores (three Bodipy and one truxene dyes) are embedded within the star-shaped structure of the title compound. Moreover, the bodipy subunits used absorb at different wavelengths: this allows **1** to absorb a large fraction of UV and visible radiation. Electronic absorption spectroscopy and steady-state and time-resolved luminescence experiments show that efficient and fast directional cascade energy migration takes place in **1**, which behaves as an efficient artificial light-harvesting antenna of novel composition.

The target multichromophoric platform **1** comprising separate Bodipys' residues, hereafter abbreviated **A**, **B**, and **C**, was prepared in three steps from the preformed truxene platform **T** bearing three iodo functions (Scheme 1). The key tenet of the synthetic strategy is the step-by-step introduction of the ethynyl grafted yellow dye **A**, blue dye **B**, and green dye **C**. All reactions are promoted by Pd(0), and the first step provides **TA** in 40% yield. Under such conditions, di- and trisubstituted compounds are isolated as side products. The iterative cross-coupling between **TA** and successively **B** and **C** provides dye **1** in 27% overall yield. Likewise cross-coupling between **T** and dye **B** or **C** provides the reference dye **TB** or **TC** in 22 and 19% yields, respectively.

Scheme 1[a]

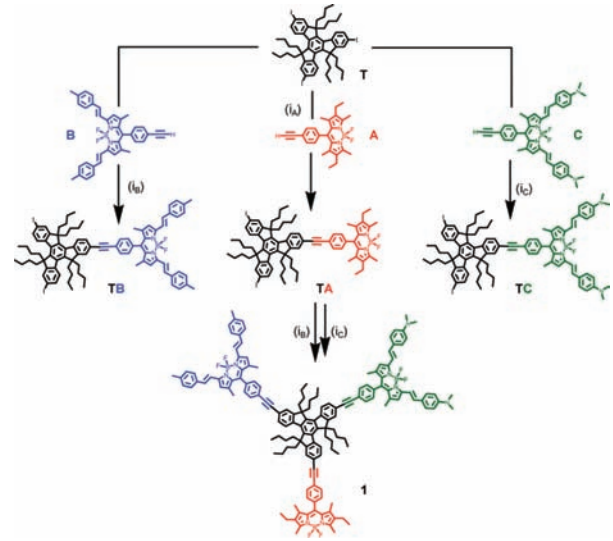

[a] (i) $[Pd(PPh_3)_4]$ (10 mol%), Et_3N, C_6H_6, 60 °C, 18 h. For **TA** 40%, for **TB** 22%, for **TC** 19%, and for **1**, 27% global yield.

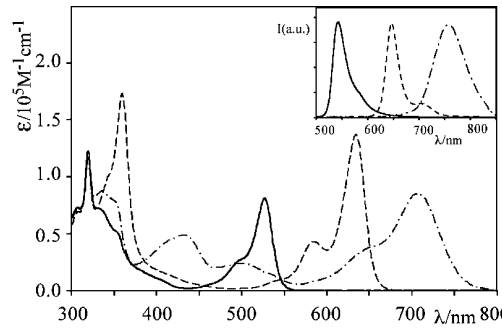

Figure 1. Absorption and emission (inset) spectra of **TA** (solid line), **TB** (dashed), and **TC** (dotted) in dichloromethane.

The truxene derivative **T** exhibits (see Table 1 and Supporting Information (SI)) a strong UV absorption at wavelengths shorter than 330 nm and a structured emission maximizing at 362 nm ($\tau = 0.5$ ns, $\Phi = 0.02$). The Bodipy dyes **A**, **B**, and **C** show absorption spectra dominated by the Bodipy-based visible bands,[3] whose maximum moves to the red going from **A** to **C**. All three bodipy dyes exhibit an intense emission, with lifetimes in the nanosecond time scale (Table 1).

The three bichromophoric species **TA**, **TB**, and **TC** have absorption spectra which are roughly the sum of those of their

[†] ECPM-CNRS.
[‡] Università di Messina.

10.1021/ja9015364 CCC: $40.75

Table 1. Absorption and Luminescence Data[a]

compound	absorption, 298 K λ_{max}/nm (ε/M^{-1} cm^{-1})	luminescence, 298 K λ_{max}/nm	Φ	τ/ns
T	316 (130 000)	362	0.02	0.5
A	528 (75 200)	540	0.92	4.3
B	636 (140 700)	647	0.74	4.4
C	709 (90 300)	767	0.18	2.0
TA	528 (78 000)	540	0.90	4.5
TB	636 (142 000)	647	0.70	4.4
TC	710 (89 100)	767	0.18	2.2
1	710 (92 000)	767[b]	0.18	2.2

[a] In dichloromethane. The reported quantum yields have been obtained by exciting at the lowest-energy absorption band of the compound. [b] Weak contribution at 540 and 647 nm (see Figure 4).

subunits (Table 1, Figure 1); however, the emission spectra only show the corresponding Bodipy emission, regardless of the excitation wavelength, demonstrating that efficient energy transfer (ET) from the truxene subunit to the Bodipy subunit(s) occurs, as supported by excitation spectra, recorded at the Bodipy emission wavelengths, which overlap with the corresponding absorption spectra. Since there is no trace of **T** emission in the three bichromophoric species, the rate constant for ET processes must be significantly faster than the luminescence lifetime of free **T**, i.e., $>2 \times 10^9$ s^{-1}. The mechanism of such ET processes is most likely electron exchange, since the equation for the Forster-type Coulombic mechanism[8] gives much slower rate constants ($<10^7$ s^{-1}).

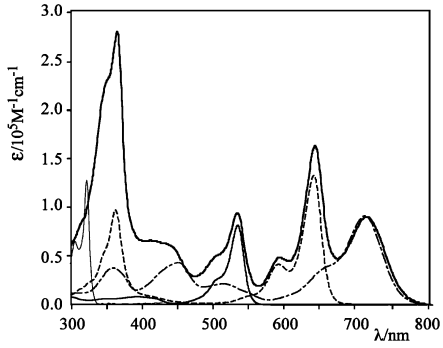

Figure 2. Absorption spectrum of **1** (solid, bold line) in dichloromethane. The spectra of the various components **T**, **A**, **B**, and **C** are shown in the background for comparison.

The absorption spectra of **1** (Figure 2) includes contributions from all the four chromophoric subunits: absorption in the 480−560 nm region is contributed by the **A** subunit, absorption in the 560−680 nm is mainly due to the **B** subunit, and absorption in the 400−480 nm and at wavelengths longer than 700 nm is attributed to the **C** subunit. At wavelengths shorter than 330 nm the absorption of truxene core prevails. Whereas the spectrum of **1** in the visible is the sum of the individual components, some deviation occurs in the UV: this can be due to electronic changes on passing from the iodo-substituted **T** to truxene core in **1**.

The emission spectrum of **1** is dominated by a band peaking at 767 nm, corresponding to the emission of the **C** subunit (Table 1, Figure 3), at any excitation wavelength. This indicates that the excited states of **A** and **B** subunits (and also of the truxene core) are efficiently quenched in **1** by the presence of the lower-lying **C** subunit. The quenching mechanism is ET, since the excitation spectrum of **1**, recorded at 770 nm, fairly overlaps with the absorption spectrum (see Figure 3, inset). However, minor contributions from **A** and **B** subunits emission can be seen at 540 and 645 nm, respectively; as expected, the percentage of such contributions to the overall emission spectrum slightly changes with the excitation wavelength. To roughly evaluate the efficiency of the ET processes, the quantum yields of the 540 and 645 nm emissions of **1** have been compared to the corresponding quantum yields of **TA** and **TB**, both exciting in the UV region at 316 nm (the wavelength at which truxene absorption is maximized compared to Bodipys absorption) and at the absorption maxima of **TA** and **TB**. In any case, the emission quantum yields of the **A** and **B** subunits in **1** are between 1% and 2.5% compared to the unquenched emissions in **TA** and **TB**. The fluorescence lifetimes of **1**, performed at various emission wavelengths, confirm the close-to-quantitative quenching results obtained by steady-state determination: the emission lifetime of the 767 nm emission is 2.2 ns, in agreement with the emission lifetime of **TC**, whereas it was impossible to determine lifetimes for the 540 and 645 nm residual emissions, indicating that the residual emission lifetimes are shorter than excitation pulse (150 ps). These results indicate that a quite efficient, directional energy migration takes place in **1**, with at least 97.5% (depending on excitation wavelength) of the UV and visible excitation light[9] leading to formation of the lowest-lying singlet excited state of the subunit **C**, which plays the role of the energy trap of **1**.

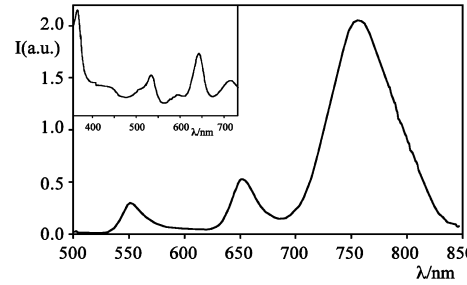

Figure 3. Emission spectrum of **1**; λ_{exc}, 316 nm. Inset: excitation spectrum of **1**; emission wavelength, 770 nm.

The Förster equation has been used for calculating ET rate constants for the individual steps **A** → **B**, **B** → **C**, and **A** → **C** in **1**, by using as models the absorption and emission spectra of **TA**, **TB**, and **TC**.[10] The results are shown in Table 2 (see also SI). Moreover, we estimated ET rate constants for the step **B** → **C** and for the global ET from **A** to **B** and **C** by taking advantage of the residual quantum yield emissions of **B** and **A** subunits in **1** (Table 2).[11] The rate constants calculated by both methods are in fair agreement, so we can suggest that Förster ET is the operating mechanism for interbodipy ET in **1**.

To estimate the contributions of individual **A** → **B** and **A** → **C** ET steps to the decay of the **A**-based excited state in **1** by the quantum-yield-based method, we performed a comparison between the **A**-based emission quantum yields of model compounds $\mathbf{TAB_2}$, $\mathbf{TA_2C}$ (prepared for this purpose, see Figure 4) and **TA**, on exciting directly the **A** subunit. Comparison between the **A** emission quantum yields of $\mathbf{TAB_2}$ and **TA** gives information on the **A** → **B** ET, and comparison between the **A**-based emission quantum yields of $\mathbf{TA_2C}$ and **TA** gives hints on the **A** → **C** ET. By applying the above-described quantum-yield-based method, we obtained rate constant values of 5.5×10^{10} s^{-1} (efficiency, 99.6%) for the **A** → **B** ET[12] and of 2.2×10^9 s^{-1} (efficiency, 90.0%) for the **A** → **C** ET. Although such ET rates are obtained for model systems, the structural similari-

ties between all these species allow us to use them as reasonable model values for the ET steps occurring in **1**.[13] The difference between individual **A** → **B** and **A** → **C** ET rate constants tends to suggest that a "circular" order (from **A** to **B** and finally to **C** subunits) in the energy migration pathway within **1** could be active.

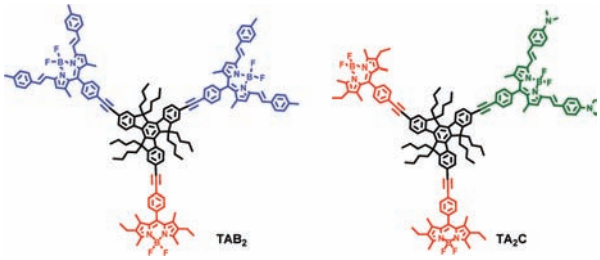

Figure 4. Structural formulas of the models.

Table 2. Rate Constants for ET Steps in **1** and Models (CH_2Cl_2, 298 K)

ET step	k_{en} (Φ based)	efficiency[a]	k_{en} (Förster)	efficiency[b]
A → **B**	5.5×10^{10} s^{-1} [c]	99.6%[c]	3.6×10^{10} s^{-1}	99.4%
B → **C**	2.2×10^{10} s^{-1}	98.0%	9.9×10^{10} s^{-1}	99.8%
A→ **C**	2.2×10^{9} s^{-1} [c]	90.0%[c]	1.8×10^{10} s^{-1}	98.3%
A → **B** + **A** → **C**	2.2×10^{10} s^{-1}	98.0%		

[a] From quantum yields data. It is the efficiency of the ET step, calculated as the percentage of emission quantum yield of the donor which is quenched on passing from the bichromophoric **TA** and **TB** species to the star-shaped species **1**, on exciting directly the donor chromophore at its absorption maximum. [b] The efficiency of ET, according to Förster calculations. [c] Calculations from direct experimental data of **1** of separated **A** → **B** and **A** → **C** ET rate constants are not possible; estimations have been made by experiments performed on model species and are reported in the text.[11]

In conclusion, a novel supramolecular multichromophoric array **1** has been prepared. The soluble and well-characterized dye **1** has a star-shaped structure, with Bodipy dyes arranged around a truxene core, which has for the first time been functionalized with three different modules. Luminescence experiments have shown that **1** features highly efficient and fast energy migration processes. Both Dexter-type (from the truxene core to the peripheral Bodipys) and Förster-type (between the peripheral Bodipy subunits) mechanisms likely contribute to the overall energy migration process. Current work is dedicated to kinetically resolve the various ET steps by ultrafast spectroscopy and to extend the study to advanced star-shaped multichromophoric species in which the directionality of the cascade ET process is controlled by addition of protons, cations, or anions.

Acknowledgment. This work was supported by the CNRS, MIUR (PRIN project) and the Ministère de la Recherche et des Nouvelles Technologies. We are indebted to Dr. Gilles Ulrich for providing us a sample of compound **A**.

Supporting Information Available: Detailed synthesis and characterization and NMR spectra of all the systems; absorption and emission spectra of **T**; equipment used; methods used for calculating ET rate constants. This material is available free of charge via the Internet at http://pubs.acs.org.

References

(1) (a) Balzani, V.; Credi, A.; Venturi, M. *Molecular Devices and Machines - Concepts and Pespectives for the Nanoworld*, 2nd ed.; Wiley-VCH: Weinheim, 2008. (b) Serin, J. M.; Brousmiche, D. W.; Fréchet, J. M. J. *Chem. Commun.* **2002**, 2605. (c) Weil, T.; Reuther, E.; Müllen, K. *Angew. Chem., Int. Ed.* **2002**, *41*, 1900. (d) Cotlet, M.; Vosch, T.; Habichi, S.; Weil, T.; Müllen, K.; Hofkens, J.; De Schryver, F. *J. Am. Chem. Soc.* **2005**, *127*, 9760.

(2) This topic is too vaste to be exhaustively cited. For some examples, see: (a) Gust, D.; Moore, T. A.; Moore, A. L. *Acc. Chem. Res.* **2001**, *34*, 40. (b) Grätzel, M. *Nature (London)* **2001**, *414*, 338. (c) Alstrum-Acevedo, J. H.; Brennaman, M. K.; Meyer, T. J. *Inorg. Chem.* **2005**, *44*, 6802. (d) Nakamura, Y.; Aratani, N.; Osuka, A. *Chem. Soc. Rev.* **2007**, *36*, 831. (e) Armaroli, N.; Balzani, V. *Angew. Chem., Int. Ed.* **2007**, *46*, 52.

(3) (a) Loudet, A.; Burgess, K. *Chem. Rev.* **2007**, *107*, 4891. (b) Ulrich, G.; Ziessel, R.; Harriman, A. *Angew. Chem., Int. Ed.* **2008**, *47*, 1184.

(4) (a) Kurack, K.; Kollmannsberger, M.; Daub, J. *Angew. Chem., Int. Ed.* **2001**, *40*, 385. (b) Yilmaz, M. D.; Bozdemir, O. A.; Akkaya, E. U. *Org. Lett.* **2006**, *8*, 2871. (c) Saki, N.; Dinc, T.; Akkaya, E. U. *Tetrahedron* **2006**, *62*, 2721. (d) Zhang, X.; Xiao, Y.; Qian, X. *Org. Lett.* **2008**, *10*, 29.

(5) Nastasi, F.; Puntoriero, F.; Campagna, S.; Diring, S.; Ziessel, R. *Phys. Chem. Chem. Phys.* **2008**, *10*, 3982, and references therein.

(6) (a) Yuan, M. S.; Fang, Q.; Liu, Z. Q.; Guo, J. P.; Chen, H. Y.; Yu, W. T.; Xue, G.; Liu, D. S. *J. Org. Chem.* **2006**, *71*, 7858. (b) Yuan, M. S.; Liu, Z. Q.; Fang, Q. *J. Org. Chem.* **2007**, *72*, 7915.

(7) (a) Sun, Y.; Xiao, K.; Liu, Y.; Wang, J.; Pei, J.; Yu, G.; Zhu, D. *Adv. Funct. Mater.* **2005**, *15*, 815. (b) Pei, J.; Wang, J. L.; Cao, X. Y.; Zhou, X. H.; Zhang, W. B. *J. Am. Chem. Soc.* **2003**, *125*, 9944.

(8) (a) Balzani, V.; Scandola, F. *Supramolecular Photochemistry*; Horwood: Chichester, U.K., 1991; Chapter 6. (b) Braslavsky, S. E.; Fron, E.; Rodriguez, H.; San Roman, E.; Scholes, G. D.; Schweitzer, G.; Valeur, B.; Wirz, J. *Photochem. Photobiol. Sci.* **2008**, *7*, 1444.

(9) The 97.5% of excited light leading to the **C** singlet state is the lower limit for energy migration efficiency as a function of excitation wavelength and is obtained at excitation wavelengths corresponding to the maxima of **A** and **B** subunits.

(10) This approach is made possible by the supramolecular nature of **1** as evidenced in Figures 2 and 3.

(11) See SI for further experimental details. However, the ET rate constants calculated by the quantum yield method should be considered with care, because of the large uncertainty of quantum yields determinations, particularly in the case of low quantum yields.

(12) The different number of **B** acceptor chromophores in $\mathbf{TAB_2}$ and **1** is considered. The reported values consider one acceptor, as is the case in **1**.

(13) The **A** → **B** ET rate constant estimation is in agreement with that obtained by Förster equation and also with the global (**A** → **B** plus **A** → **C**) decay of **A** in **1** (Table 2). On the contrary, the rate constant for **A** → **C** ET estimated by $\mathbf{TA_2C}$ quantum yield data is significantly lower than that calculated by Förster theory. The origin of this disagreement could lie in the nature of the excited state of the **C** dye. Such a state is expected to have a significant CT nature, involving the dimethylamino group, so the donor−acceptor distance value used in the Förster calculation is probably shorter than the effective one.

JA9015364